A MECHATRONIC APPROACH TO THE CONTROL OF MACHINE TOOLS

Gianni Ferretti, Francesco Lucchini, GianAntonio Magnani, Paolo Rocco

Politecnico di Milano,
Dipartimento di Elettronica e Informazione,
Piazza Leonardo da Vinci, 32, 20133 Milano, Italy

Abstract: One of the most common sources of performance limitation in the control of machine tools is associated to the resonant dynamics of the drive train, induced by the elasticity in some components. The design of the control system should guarantee a damped behavior of the load position, both in the setpoint response and in the rejection of the disturbances arising from the machining operation. In this paper reference is made to the common P/PI control scheme, and stability analysis with adimensional parameters is first discussed. Tuning of the controller gains is then set as a problem of minimizing the H_∞ norm of some closed loop transfer functions, for which closed form approximations are also given. The methodology is finally applied to the design of the control system for an axis of a milling machine, whose virtual prototype developed in the Dymola environment is also discussed.

Keywords: Machines; mechanical systems; performance indices; PID control; simulation; stability analysis.

1. INTRODUCTION

Virtual prototyping (Ferretti, *et al.*, 2004) of machine tools and other mechanical systems consists in the use of detailed multi-domain mathematical models assembled and simulated with appropriate software packages. These models allow to assess the behavior of the components and of the overall system from the dynamical standpoint, addressing, for example, the vibration reduction problem. Significant advantages in terms of cost reduction and shorter development times are expected from the adoption of these CAD tools. The virtual prototype actually allows to simulate experiments within the software environment. It is therefore possible to evaluate alternatives in the (mechanical or electronic) design with limited costs compared to physical experiments.

On the other hand such an approach only allows assessment of design choices and does not usually give indications on the direction to be followed. It would then be advisable that virtual prototyping environments or, more in general, that software packages for computer aided design, offered, as it is common in other contexts, guided procedures for the optimization of certain cost functions.

A first step in this direction, in the mechatronic context, might consist in making reference to simplified (linear and lumped parameters) models of the mechanical dynamics in closed loop with the control, over which performance indices can be easily defined and computed. These performance indices can then be related to the physical and geometrical parameters, on one hand, and to the controller gains, on the other.

The research in this field has not yet reached maturity since, apart from some preliminary results (Ferretti, *et al.*, 2003), systematic tools have not yet been presented that duly take into account the different and sometimes contrasting goals that the design of the motion control for a servomechanism should achieve (from rapid positioning to efficient rejection of disturbances arising during machining). On the other hand, the lively interest of both industrial and academic worlds for the issues related to the mechatronic design of systems is witnessed by

a somewhat wide body of literature (Ferretti, *et al.*, 2003), (Hewit, 1996), (Coelingh, *et al.*, 2002), (Reinhart and Weissenberger, 1999), (Van Amerongen, 2003). More theoretical approaches have been pursued in (Goodwin *et al.*, 2003) and (Middleton *et al.*, 1999).

In this paper a load behavior concerned control of two-mass system is discussed. The classical control scheme used in machine tool industry, namely a PI (proportional-integral) controller closed on the motor velocity (actually obtained through numerical differentiation of the motor position) and a proportional controller closed on the load position, is assumed. A study on the stability of such a control scheme is first presented, making reference to all normalized (adimensional) parameters, which enhances generality of the conclusions.

The performance limitations of the P/PI control scheme are then quantified through the H_∞ norms of two closed loop transfer functions, from position setpoint to load position and from load side torque disturbance to load position, respectively. Simple expressions for these performance indices are given, that depend on physical parameters of the system, as well as on a free control design parameter (the nominal bandwdith of the velocity loop, conveniently normalized). Since mechanical and control parameters contribute to the performance index, the relation supports *codesign* (mechatronic design) of the servo system.

As an application example, the case of a milling machine is discussed. A virtual prototype of an axis of the machine has been developed, paying particular attention to the model of the cutting forces arising at the contact between the tool and the piece. These forces play the role of disturbances on the load side for the motion control system. The elasticity of the components of the drive train (a belt stage and a ball-screw stage) has been analyzed in detail, too, since flexibility of the transmission is recognized as one of the main limiting factors of the performance. The simulator has been developed in the Dymola environment, supporting the physical modeling language Modelica (Ferretti, *et al.*, 2004).

The analysis developed in the first part of the paper is applied to the milling machine example, for which the curves representing the H_∞ norms of the two closed loop transfer functions are plotted and used in order to design the motion controller. Simulation results are also shown.

2. SYSTEM MODEL

The dynamic behavior of an axis of a machine tool is usually well represented by a two-mass model, where in the first and in the second masses all the inertial effects of the bodies rotating at the motor velocity and at the load velocity, respectively, are concentrated, while a spring and damper capture the elastic properties of the transmission chain.

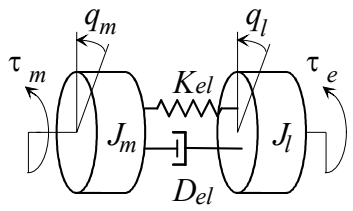

Fig. 1 Two mass model.

We consider thus a servo system where the motor is connected to the load through an elastic transmission, characterized by a stiffness K_{el} and a damping D_{el}. In Fig. 1 a sketch of the system is drawn. The first flywheel represents the inertia (J_m) of the motor, the second one is associated to the load, whose inertia is J_l. The torque τ_m is applied to the rotor, and the motion is described by the position coordinates q_m and q_l with respect to a fixed reference. Assuming the current loop bandwidth sufficiently high, the torque τ_m can be directly assumed as an input to the system. An external torque τ_e might be applied on the load side as an input signal as well.

The relevant transfer functions for the two-mass system under control are the following ones:

$$G_{11}(s)=\frac{q_m(s)}{\tau_m(s)}=\frac{\mu}{s^2}\frac{1+2\frac{\zeta_z s}{\omega_z}+\frac{s^2}{\omega_z^2}}{1+2\frac{\zeta_p s}{\omega_p}+\frac{s^2}{\omega_p^2}} \tag{1}$$

$$G_{21}(s)=\frac{q_l(s)}{\tau_m(s)}=\frac{\mu}{s^2}\frac{1+2\frac{\zeta_z s}{\omega_z}}{1+2\frac{\zeta_p s}{\omega_p}+\frac{s^2}{\omega_p^2}} \tag{2}$$

$$G_{12}(s)=\frac{q_m(s)}{\tau_e(s)}=\frac{\mu}{s^2}\frac{1+2\frac{\zeta_z s}{\omega_z}}{1+2\frac{\zeta_p s}{\omega_p}+\frac{s^2}{\omega_p^2}} \tag{3}$$

$$G_{22}(s)=\frac{q_l(s)}{\tau_e(s)}=\frac{\mu}{s^2}\frac{1+2\frac{\zeta_z s}{\omega_z}+\frac{s^2}{\rho\omega_z^2}}{1+2\frac{\zeta_p s}{\omega_p}+\frac{s^2}{\omega_p^2}} \tag{4}$$

where $\mu=1/(J_m+J_{lr})$, ω_z, ζ_z are the natural frequency and damping factor of the zeros, respectively, while ω_p, ζ_p are the natural frequency and damping factor of the poles of the system, respectively. These parameters are related to the physical ones by the following equations:

$$\omega_z=\sqrt{\frac{K_{el}}{J_{lr}}} \tag{5}$$

$$\xi_z=\frac{D_{el}}{2}\frac{1}{\sqrt{J_{lr}K_{el}}} \tag{6}$$

$$\frac{\omega_p}{\omega_z} = \frac{\zeta_p}{\zeta_z} = \sqrt{1+\rho} > 1 \qquad (7)$$

where $\rho = J_{lr}/J_m$ is the so called inertia (or mass) ratio.

Notice that all the quantities defined on the load side have been related to their counterparts on the motor side, by means of convenient scaling through the gear ratio n. This is useful for analysis as it allows to work with variables and parameters that can be easily compared. Thus q_l stands for the load position multiplied by the gear ratio, τ_e for the torque on the load side divided by the gear ratio, while the inertia moment on the load side reduces to $J_{lr} = J_l / n^2$.

3. STABILITY OF A P/PI CONTROLLER

A classical control scheme used in machine tools is the so called P/PI controller: a PI controller is closed on the motor velocity (actually obtained through numerical differentiation of the position) while an outer proportional loop is closed on the load position (Fig. 2). A velocity feedforward is also used to speed up the setpoint response. Notice that in the nominal rigid case where the motor and load positions (q_m and q_l) do not differ, this control scheme is equivalent to a PID controller closed on the position error. The zeros of this equivalent PID controller coincide with the zero of the PI on the velocity and with the gain k_{pp}, as it can be quite easily verified.

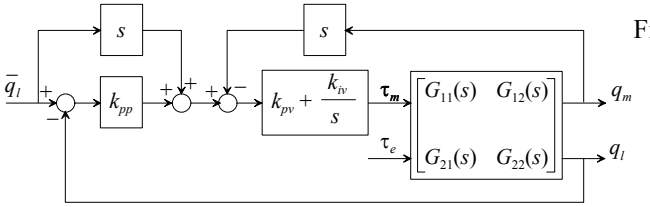

Fig. 2 P/PI control system.

Let us first study the stability properties of the control scheme. For this, the closed loop polynomial can be computed, normalizing all terms with suitable algebraic manipulations. The result is a polynomial in the normalized variable $p=s/\omega_z$, that takes the form (8):

$$\chi(p) = \alpha_0 p^5 + \alpha_1 p^4 + \alpha_2 p^3 + \alpha_3 p^2 + \alpha_4 p + \alpha_5 \qquad (8)$$

where the expressions for the adimensional coefficients α_i are given in Table I. The following adimensional control gains have been introduced:

$$\gamma_{pp} := \frac{k_{pp}}{\omega_z}, \quad \gamma_{pv} := \frac{k_{pv}\mu}{\omega_z}, \quad \gamma_{iv} := \frac{k_{iv}\mu}{\omega_z^2} \qquad (9)$$

together with the adimensional physical parameters ζ_z and ρ. If the working hypothesis is enforced that both the zeros of the equivalent PID are equal to the zero of the PI on the motor velocity, i.e. $\gamma_{iv} = \gamma_{pp}\gamma_{pv}$, and a unitary inertia ratio (ρ=1) is assumed, stability regions can be plotted in the planes formed by two out of three adimensional gains, at varying damping factor ζ_z. These plots are reported in Fig. 3, 4, 5 and show that the stability regions enlarge at increasing damping factor ζ_z of the transmission (ζ_z ranges from 0.01 to 0.5).

Table 1 Normalized coefficents of (8)

α_0	$(1+\rho)^{-1}$
α_1	$2\zeta_z + \gamma_{pv}$
α_2	$1 + 2\zeta_z\gamma_{pv} + \gamma_{iv}$
α_3	$\gamma_{pv}(1 + 2\zeta_z\gamma_{pp}) + 2\zeta_z\gamma_{iv}$
α_4	$\gamma_{pp}\gamma_{pv} + 2\zeta_z\gamma_{pp}\gamma_{iv} + \gamma_{iv}$
α_5	$\gamma_{pp}\gamma_{iv}$

.

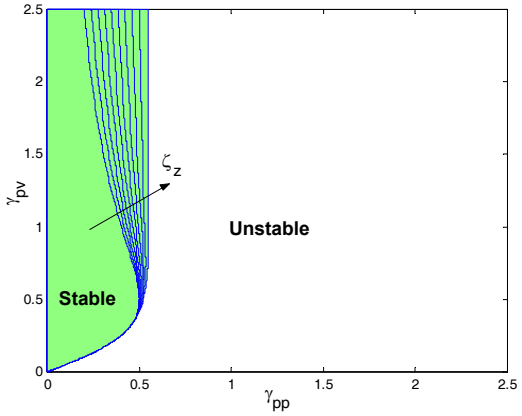

Fig. 3 Stability region in the plane γ_{pp}, γ_{pv}.

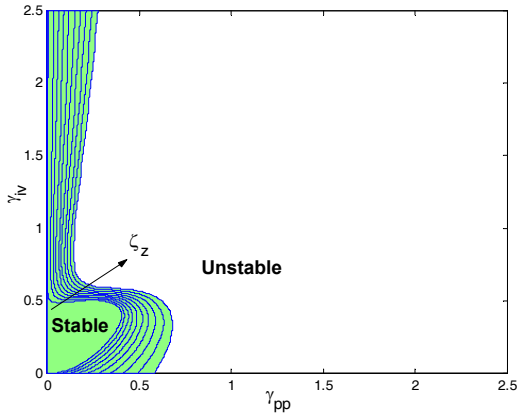

Fig. 4 Stability region in the plane γ_{pp}, γ_{iv}.

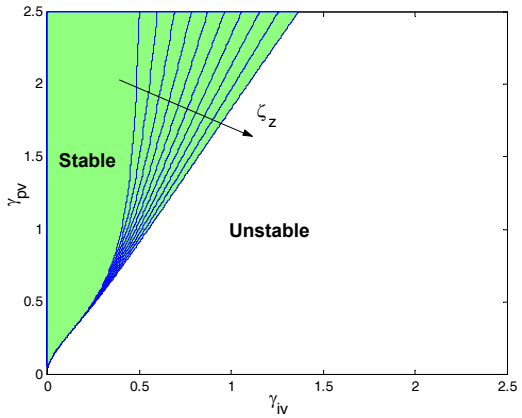

Fig. 5 Stability region in the plane γ_{iv}, γ_{pv}.

The adimensionality of the parameters used to produce these plots make them immediately usable in order to select a set of control gains well inside the stability region.

4. PERFORMANCE LIMITATIONS ON A P/PI CONTROLLER

Consider again the block diagram of the control system in Fig. 2. In this Section we analyze the effects on the load motion of an increasingly high bandwidth controller, deriving a quantitative measure of the loss of performance on the load side.

In order to further reduce the degrees of freedom of the control system, a second hypothesis is enforced here, namely that the zeros of the equivalent PID controller, already supposed to be equal, are placed one decade before the nominal crossover frequency of the velocity loop, ω_c, computed with reference to a rigid system. This frequency is therefore the actual free parameter of the controller. It can be easily approximated observing that in nominal conditions, i.e. with a rigid transmission, the velocity loop transfer function is:

$$L(s)=\left(k_{pv}+\frac{k_{iv}}{s}\right)\frac{\mu}{s} \qquad (10)$$

The nominal crossover frequency can then be rather well approximated considering only the high frequency part of the transfer function, thus letting:

$$\omega_c = k_{pv}\mu\,, \qquad (11)$$

or, in normalized coordinates:

$$\tilde{\omega}_c = \frac{\omega_c}{\omega_z} = \gamma_{pv}\,. \qquad (12)$$

It is common wisdom among users of machine tool controllers that increasing ω_c (or equivalently increasing "the gain" of the velocity loop) the machine performance improve in terms of motor response but vibrations may occur. A trade off is usually achieved on an experimental basis, once the servo has been assembled. In a large number of motion control systems it results $\tilde{\omega}_c$<1.

These empirical circumstances can be formalized deriving a quantitative relation between ω_c and the amount of oscillation of the load. The latter is expressed through the H_∞ norm of two transfer functions: the first one is from the load position setpoint $\bar{q}_l$ to the load position q_l, the second one is from the external torque τ_e to the same load position q_l. As the H_∞ norm of a transfer function measures the peak of the amplitude of the frequency response, the higher this norm is, the more resonant the system is. The reason for evaluating the H_∞ norm of both the closed loop transfer functions is that the study of just the setpoint response (carried out for example in (Ferretti, *et al.*, 2003)) might be incomplete, in all those cases where significant disturbances arise at the load side, as for example a milling machine like the one described in next Section.

Assigning suitable values to the damping factor ζ_z of the transmission and to the inertia ratio ρ, and exploiting the relations among controller gains previously introduced, the H_∞ norms can be numerically computed and plotted versus the normalized crossover frequency $\tilde{\omega}_c$. This is done in Fig. 6 for the transfer function from the position setpoint $\bar{q}_l$ and in Fig. 7 for the transfer function from the external torque τ_e. The values ζ_z=0.038 and ρ=1.8 have been adopted.

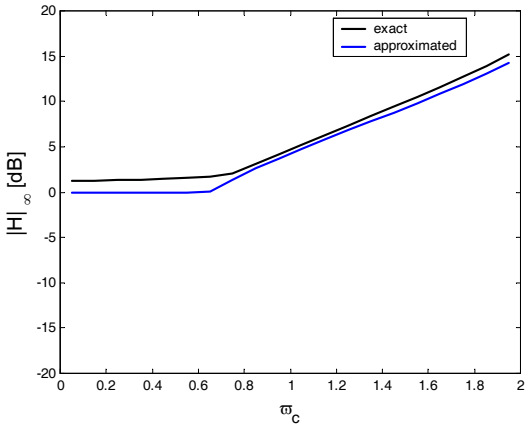

Fig. 6 H_∞ norm of the transfer function from the position setpoint.

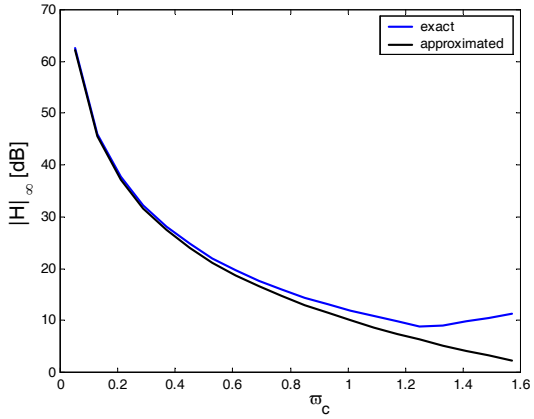

Fig. 7 H_∞ norm of the transfer function from the external torque.

Both the figures show the plots of some approximating functions too. These functions are obtained with the techniques described in detail in (Lucchini, 2004), where they have been derived also for different control configurations. Their expressions is here reported:

$$\left|\frac{q_l}{\bar{q}_l}\right|_\infty \approx \tilde{\omega}_c \sqrt{\frac{1+0.1\tilde{\omega}_c^2}{\left(\frac{\rho}{1+\rho}\right)^2 + 0.1\tilde{\omega}_c^4 + 2\zeta_z\frac{\rho}{1+\rho}\tilde{\omega}_c - 0.2\frac{\rho}{1+\rho}\tilde{\omega}_c^2 - 0.4\zeta_z\tilde{\omega}_c^3}} \qquad (13)$$

$$\left|\frac{q_l}{\tau_e}\right|_\infty \approx 5\frac{\frac{\rho}{1+\rho}}{\tilde{\omega}_c^2} \qquad (14)$$

The approximating functions fit rather well the actual plots, apart from the approximation in Fig. 7 for

higher values of $\tilde{\omega}_c$. While the actual (exact) plots can be derived with a modest programming and computational effort, these closed form approximations might be useful in order to dimension the servo system. Notice that this dimensioning is to be intended in a mechatronic sense: the parameters to be adjusted might be the controller gains, ultimately expressed by the crossover frequency $\tilde{\omega}_c$, but also the mechanical data (like the inertia ratio ρ and the damping factor ζ_z) might be changed in order to minimize the cost functions.

5. APPLICATION TO A MILLING MACHINE

The milling machine studied in this paper has a "T" configuration and is used to work pieces of large dimensions and weight. The structure is made of steel electrically welded and thermally stabilized. The axes move over low pressure hydrostatic guides. In Fig. 8 a scheme of the machine can be found, where the names of the axes are also reported.

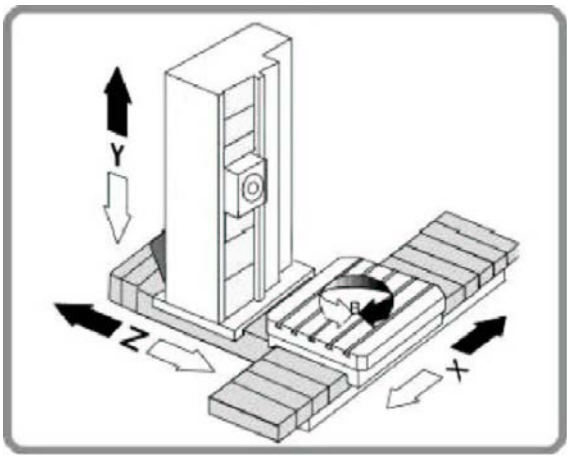

Fig. 8 The milling machine studied in this work.

Only the Z axis is here considered, where reference is made to a frontal milling operation. An auxiliary head is mounted on the machine, allowing to rotate by 90° the spindle in order to put it in the vertical direction. The X and Y axes are not considered in the model. Actually these axes are not used in the machining operation: once they are placed in the correct position, they are mechanically braked.

The drive train of the Z axis is realized coupling a brushless motor to a transmission having two stages: the first one is a belt, the second one is a ball-screw coupling (Fig. 9).

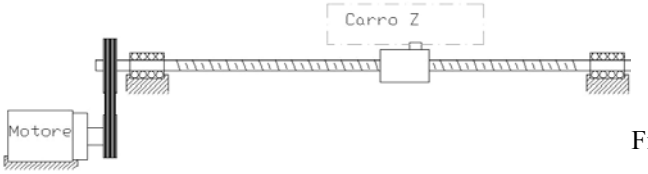

Fig. 9 Scheme of the Z axis.

A detailed simulation model of the milling machine has been assembled in the Dymola environment: Fig. 10 shows the top level view of the simulator. Particularly critical, but not detailed here, is the modelling of the cutting forces at the interaction between the cutter and the piece. The model has been validated against experimental data found in the literature (Cheng, *et al.*, 1997).

In order to make use of the results summarized in Section 4, a two-mass model of the transmission has been derived. Only the first natural frequency of the system has been retained, that is actually associated to the ball-screw stage rather than to the belt stage. With the physical values of this two-mass system (ζ_z=0.089 and ρ=0.77), the H_∞ norms plotted versus the normalized crossover frequency $\tilde{\omega}_c$ are reported in Fig. 11.

It is apparent that values of $\tilde{\omega}_c$ slightly higher than 1 might be a good choice, as the H_∞ norm of the transfer function from the torque disturbance presents a minimum, while the norm of the transfer function from the position setpoint is not excessively high.

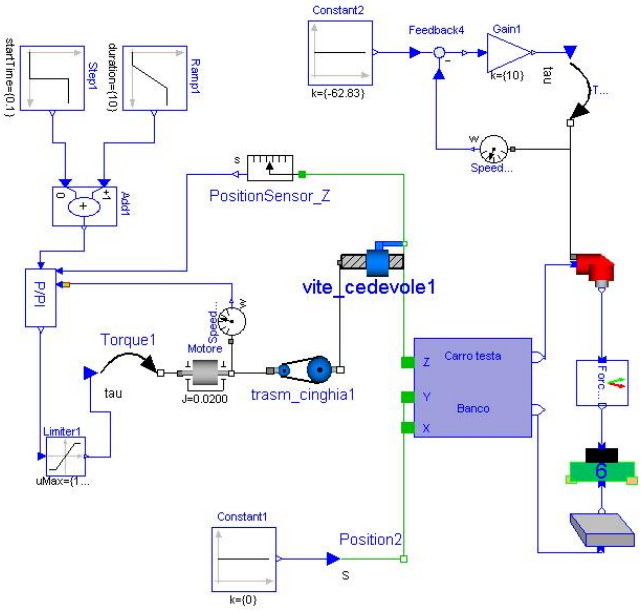

Fig. 10 Simulation model

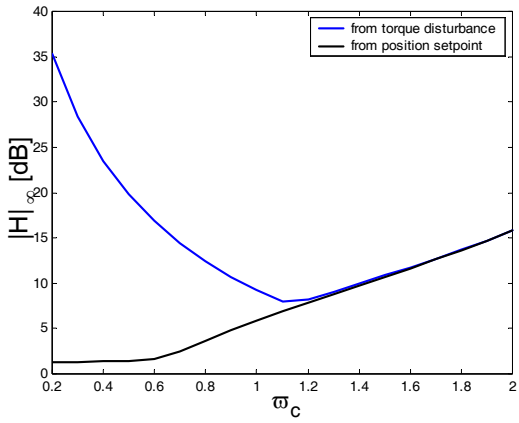

Fig. 11. H_∞ norms of the closed loop transfer functions for Z axis

Fig. 12 shows the tracking error obtained in the simulation of a milling operation, at varying normalized crossover frequency. As $\tilde{\omega}_c$ increases the disturbance rejection improves, but this improvement

is increasingly less evident. This suggests that excessively high velocity loop bandwidths are not advisable, also considering that besides the transient related to the first contact, significant differences do not emerge in the steady state behavior during machining. As an example, Fig. 13 reports the errors, conveniently translated in order to facilitate the comparison, in the two cases $\tilde{\omega}_c$=0.5 and $\tilde{\omega}_c$=1.2. In both cases the oscillations are confined in a range not larger than 4 10^{-4}mm.

On the other hand, as the plot of H_∞ norms in Fig.11 shows, an increase in $\tilde{\omega}_c$ emphasizes the oscillatory behavior of the load as a response to setpoint variations (for example "rapid" movements made to position the tool over the piece).

All these considerations confirm that an adequate value for $\tilde{\omega}_c$ is slightly larger than 1. Based on this conclusion, and on the tuning rules summarized in Section 4, the gains of the PID controller can be properly selected.

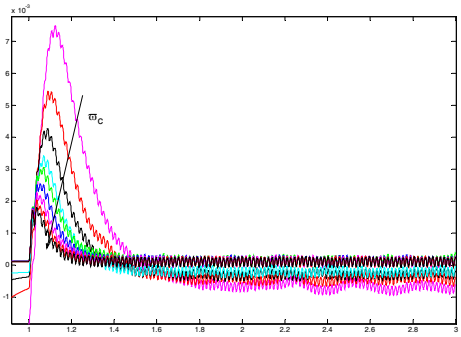

Fig. 12 Errors in a milling operation

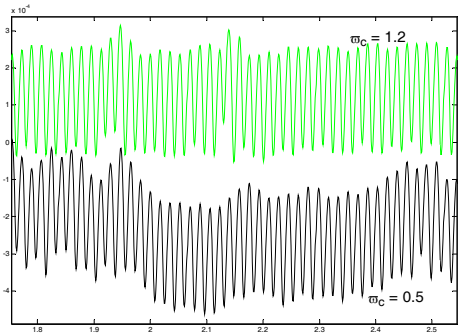

Fig. 13 Details of the errors induced by the milling forces

6. CONCLUSIONS

Virtual prototyping tools help designing machine tools, as they allow to unify the moments when decisions on the dimensioning of the mechanics, electronics and control system of the machine must be taken. The mechatronic approach is actually based on the consideration that the performance of the machine are determined by the interaction of different parts of the system, whose complexity calls for the adoption of advanced tools for modular modeling and simulation. A further step in the direction of a fully computer aided design of the machine is the availability of cost functions that guide the selection of components and tuning of the control system. The paper contributes in this field by introducing and approximating some performance indices, that assume as a measure of performance degradation the resonant behavior of the machine on the load side.

Modeling of an axis of a milling machine is an interesting benchmark for these methodologies. The related control problem, where particular relevance is assumed by the rejection of the disturbance induced by the cutting forces at the mill, might be set as the minimization of certain cost functions, achievable through a suitable tuning of the control system, but also with a design of the mechanical parts oriented towards dynamic performance.

REFERENCES

Cheng, P., J. Tsay and S. Lin (1997). A study on instantaneous cutting force coefficients in face milling, *International Journal of Machine Tools and Manufacture*, **37**, pp 1393-1408.

Coelingh, E., T. De Vries and R. Koster (2002). Assessment of mechatronic system performance at an early design stage, *IEEE/ASME Transactions on Mechatronics*, **7**, pp.269-279.

Ferretti, G., G. Magnani and P. Rocco (2003). Load behavior concerned PID control for two-mass servo systems, *Proceedings of the 2003 IEEE/ASME International Conference on Advanced Intelligent Mechatronics*, Kobe, pp.821-826.

Ferretti, G., G. Magnani and P. Rocco (2004). Virtual prototyping of mechatronic systems, *Annual Reviews in Control*, **28**, pp.193-206.

Goodwin G.C., A.R. Woodyatt, R.H. Middleton and J. Shim (1999). Fundamental limitations due to jω-axis zeros in SISO systems. *Automatica*, **35**, pp 857–863.

Hewit, J. (1996). Mechatronics design-The key to performance enhancement, *Robotics and Autonomous Systems*, **19**, pp 135-142.

Lucchini, F. (2004). A mechatronic approach to the motion control of machine tools (in Italian), Ms. Thesis, Politecnico di Milano, 2004

Middleton R. H., J.K. Ward, J.S. Freudenberg and A.R. Woodyatt (1999). Performance limitations in the feedback control of a class of resonant systems. *Proceedings IEEE Conference on Decision and Control*, pp. 1845–1850.

Reinhart, G. and M. Weissenberger (1999), Multibody simulation of machine tools as mechatronic systems for optimization of motion dynamics in the design process, *Proceedings of the 1999 IEEE/ASME International Conference on Advanced Intelligent Mechatronics*, Atlanta, pp.605-610.

Van Amerongen, J (2003), Mechatronic design, *Mechatronics*, **13**, pp. 1045-1066.